Article

Pt(IV)/Re(I) Chitosan Conjugates as a Flexible Platform for the Transport of Therapeutic and/or Diagnostic Anticancer Agents

Elisabetta Gabano [1] ![ID], **Letícia do Quental** [2], **Elena Perin** [1], **Francisco Silva** [2], **Paula Raposinho** [2], **António Paulo** [2,*] **and Mauro Ravera** [1,*] ![ID]

[1] Dipartimento di Scienze e Innovazione Tecnologica, Università del Piemonte Orientale, Viale Michel 11, 15121 Alessandria, Italy; elisabetta.gabano@uniupo.it (E.G.); elena.perin@uniupo.it (E.P.)

[2] Centro de Ciências e Tecnologias Nucleares, Instituto Superior Técnico, Universidade de Lisboa, Estrada Nacional 10 (km 139,7), 2695-066 Bobadela LRS, Portugal; leticia.a.quental@gmail.com (L.d.Q.); fsilva@ctn.tecnico.ulisboa.pt (F.S.); paular@ctn.tecnico.ulisboa.pt (P.R.)

* Correspondence: apaulo@ctn.tecnico.ulisboa.pt (A.P.); mauro.ravera@uniupo.it (M.R.); Tel.: +351-21-9946196 (A.P.); +39-0131-360252 (M.R.)

Abstract: New chitosan derivatives modified with (3-carboxypropyl)trimethylammonium chloride (**1**) and coupled with (*OC*-6-44)-diammine(4-carboxypropanoato)dichloridoethanolatoplatinum(IV) (**2**), were synthesized and their preliminary biological evaluation carried out in human tumor cells. Some of these derivatives were also loaded with a chelating ligand (**3**) that was derived from bis(quinolin-2-ylmethyl)amine to obtain chitosan-based nanoparticles for an EPR-mediated delivery of Pt(IV) prodrugs and Re(I) tricarbonyl complexes (**4**), to explore a multimodal theranostic approach to cancer. The cytotoxicity of the different chitosan conjugates (**C12**, **C123**, and **C1234**), carrying different combinations of the Pt(IV) complex, the chelator and the Re(I) complex, was evaluated in the A2780 human ovarian cancer cell line using the MTT assay. The Pt(IV)-containing nanosystems showed low to moderate cytotoxic activity (IC$_{50}$ values in the range 13.5–33.7 μM) and was comparable to that found for the free Pt(IV) complex (IC$_{50}$ = 13.7 μM). Therefore, the Pt(IV)-chitosan conjugation did not enhance the cytotoxic activity of the Pt(IV) prodrug, which certainly reflects the inefficient cellular uptake of the nanoconjugates. Nevertheless, a clearer view of their potential for the delivery of anticancer agents requires further in vivo tests because the EPR effect increases extravasation and retention within the tumor tissue, not necessarily within the tumor cells.

Keywords: theranostics; platinum prodrugs; rhenium complexes; chitosan; drug targeting and delivery

1. Introduction

In 1978, cisplatin (i.e., (*SP*-4-2)-diamminedichloridoplatinum(II)) was approved by the Food and Drug Administration as an anticancer drug. Since then, this simple Pt(II) compound has become one of the most widely used chemotherapeutic agents. It is best known for curing testicular cancer, but it is also used in the treatment of a wide range of other cancers, including lung, bladder, cervical, and ovarian cancers, alone or in combination with other drugs [1–3].

One of the major problems of Pt chemotherapeutic agents is their non-specific toxicity. Such toxic action to normal cells limits the dose of the anticancer drugs to be administered to patients, which results in unsatisfactory efficacy. To overcome this obstacle, conjugation of the drugs to suitable carriers has been studied to provide site-specificity and to increase the drug concentration at the tumor site (drug targeting and delivery, DTD).

In general, there are two possibilities of localizing a drug in the proximity of a tumor: the active and the passive ones. The former is based on coupling the drug with a macro/molecular ligand to target it to tumor tissues/cells involving specific recognition mechanisms (i.e., antigen-antibody interaction, peptide-based targeting, DNA, or RNA-based ligands, etc.). On the other hand, passive DTD uses the characteristic enhanced permeation and retention of the vasculature of the tumor (EPR effect), by which it is possible to concentrate drug-loaded nanoparticles within the tumor tissue [4]. To date, many macromolecular drugs based on EPR effect were developed, more of them are in preclinical stages, and some others are used in clinic, including liposomes, polymers, micelles, and nanoparticles [5]. Recently, the functionalization of nanostructured materials with anticancer Pt-based metallodrugs, to improve biological activities while decreasing the adverse toxicological effects, has attracted a lot of attention [6–13].

Whatever the DTD method, the release of the drug at the right moment and at the right position is crucial. In the case of square-planar Pt(II) drugs, the design of the linker between the metal moiety and the vector is of great importance. In fact, the spacer should contain a hydrolysable group to guarantee the release of the active Pt metabolite [14,15]. On the contrary, the use of octahedral Pt(IV) complexes may overcome some of the synthetic difficulties. Pt(IV) prodrugs are activated by reduction to their cytotoxic Pt(II) metabolites in the hypoxic (reducing) tumor milieu releasing the two axial ligands (Scheme 1) [16–18]. For this reason, the axial ligands on Pt(IV) complexes constitute ideal DTD vectors, since they will be released upon reduction without altering the overall activity of the final Pt(II) metabolite.
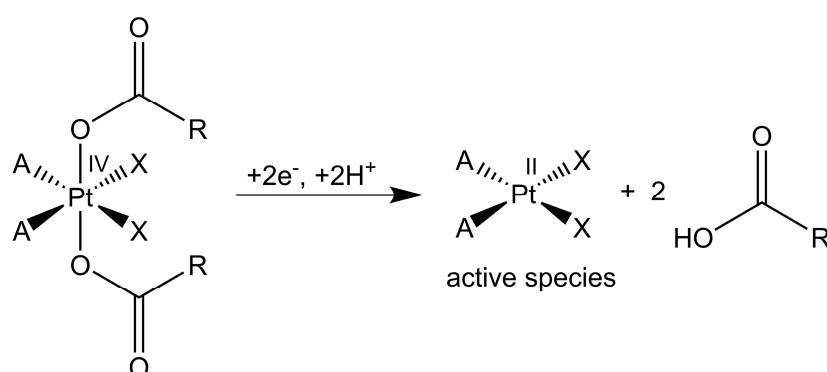

Scheme 1. General scheme of the accepted in vivo reduction of Pt(IV) prodrugs. A = amines, X = carboxylatos, chloridos, etc., R = alkyl or aryl groups.

The clinical use of cisplatin in combination with other drugs resides in the limitations of monotherapies to fully fight a complex disease, such as cancer. To attack cancer on multiple fronts, a multi-target drug may be more successful than a single component. For this reason, by combining two drugs, the probability of killing the cancer rises. So, a nanoparticle, having multiple sites able to react with several molecules, may be loaded with both a Pt-based drug and a second "weapon" (e.g., an organic drug synergistic with Pt, a radioactive isotope, etc.), and the conjugate will (should) transport and deliver both drugs simultaneously to the final destination.

Alternatively, the second drug may be replaced by an active reporter, to combine therapy and diagnostics in the same device, to treat and image efficacy with one single tool. Indeed, the development of novel agents combining diagnostic and therapeutic (theranostic) tools has emerged as a new approach to fight cancer over the last decade [19,20]. Towards this goal, isostructural M(I) (M = ^{99m}Tc or Re) tricarbonyl complexes have useful and unique features: (i) chemical robustness of the *fac*-[M(CO)$_3$]$^+$ core; (ii) well-studied coordination chemistry with a variety of chelating ligands including targeting molecules [21,22]; and, (iii) possible application in the design of metal-based cancer theranostic agents where Re complexes can be incorporated into a cytotoxic entity that will

exert a therapeutic effect, while the ^{99m}Tc congeners are part of the corresponding imaging tool for in vivo assessment of tumor accumulation. Furthermore, the Re(I) tricarbonyl complexes have also been recently explored as photosensitizers for photodynamic therapy (PDT) [23–25]. PDT is a clinically approved technique used , for instance, for the treatment of certain tumors, which involves light-induced generation of cytotoxic singlet oxygen ($^1O_2$) from endogenous $^3O_2$ and/or other reactive oxygen species (ROS), mediated by a photosensitizer. When compared with other conventional anticancer treatments, PDT has many advantages, namely spatial and temporal control and the possibility of repeated doses [19,26]. In particular, Re(I) tricarbonyl complexes with ligands derived from bis(quinolin-2-ylmethyl)amine can act as efficient photosensitizers and are endowed with luminescence properties that might also allow for the visualization of their intracellular trafficking by fluorescence microscopy [24,25].

In this work, it is reported the preparation and preliminary evaluation of the biological properties of low viscosity chitosan from shrimp shell, modified with (3-carboxypropyl)trimethylammonium chloride (**1**), coupled with (*OC*-6-44)-diammine(4-carboxypropanoato)dichloridoethanolatoplatinum(IV) (**2**) and loaded with the chelating ligand **3**, as derived from bis(quinolin-2-ylmethyl)amine for possible coordination of the Re(I) tricarbonyl moiety (Scheme 2). The idea was to use chitosan–based nanoparticles for an EPR-mediated accumulation of Pt(IV) prodrugs and Re(I) tricarbonyl complexes, to explore a multimodal theranostic approach to cancer. As a proof of principle, the coordination capability of the functionalized chitosan towards the *fac*-[Re(CO)$_3$]$^+$ was also evaluated and allowed for the synthesis of the final nanoconjugate **C1234**, as depicted in Scheme 2. To have an insight on the influence of the different payloads in the biological performance of the nanoconjugates, their cytotoxicity and cellular uptake were evaluated in the A2780 human ovarian cancer cell line.
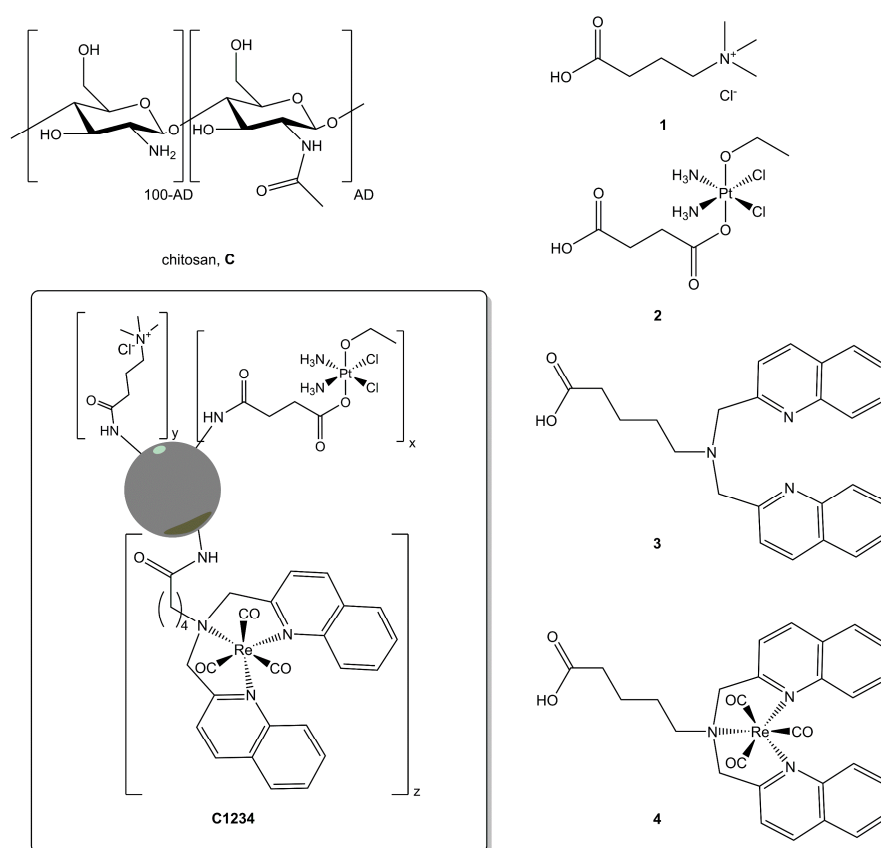
Scheme 2. Structure of chitosan **C** (AD = acetylation degree), its payloads **1–4**, and the final conjugate **C1234**.

2. Results and Discussion

2.1. Synthesis and Characterization of the Conjugates

Chitosan is a linear polysaccharide containing randomly distributed β-(1-4)-linked D-glucosamine and *N*-acetyl-D-glucosamine (Scheme 2). It is a nontoxic, biodegradable, and biocompatible [27] derivative of chitin (the second most abundant polysaccharide in nature after cellulose and one of the main components of the exoskeleton of crustaceans and insects [28]), and it is obtained by partial deacetylation of chitin amines with alkaline hydrolysis. The number of *N*-acetyl groups is expressed as molar percentage and is defined as acetylation degree (AD). When AD is lower than 60%, chitin is considered chitosan. Another characteristic that allows the evaluation the nature of the polysaccharide is the solubility in aqueous solution of organic acids (such as acetic acid), which is verified for AD lower than 50–60% [28]. Depending on acetylation degree and pH (pK_a of amino groups from 6.2 to 7.0), chitosan is a polycation with variable charge density [29]: it is protonated (and soluble) in acids with pK_a < 6.2, whereas it cannot be dissolved in water, alkaline, or physiological aqueous solutions and organic solvents [30].

The titration of chitosan to quantify the free amine functionalities (5.16 mmol –NH$_2$ groups g^{-1} chitosan, see experimental part for details) showed it was almost insoluble at physiological pH. This feature made necessary to introduce ammonium groups into this polysaccharide. In fact, to improve the water solubility of chitosan, it is possible to modify it with molecules, such as PEG or ammonium derivatives [29,31–33]. In particular, the quaternarization allows chitosan to be soluble in water, regardless of pH, only if the quaternarization degree represents at least the 25% of the total available amino groups [34]. For this purpose, (3-carboxypropyl)trimethylammonium chloride was activated with the coupling agent *N,N,N′,N′*-tetramethyl-*O*-(1*H*-benzotriazol-1-yl)uronium hexafluorophosphate (HBTU, belonging to the uronium salt family), in the presence of the tertiary amine *N,N*-diisopropylethylamine (DIPEA), and directly mixed with the nucleophilic species, i.e., the –NH$_2$ groups of chitosan (conjugate **C1**, about 30% of quaternization degree. See experimental).

To carry out the reaction between the carboxylic groups of Pt(IV) complex **2** and the amine functionalities of chitosan, the complex was initially activated in the form of succinimidyl ester with *N*-hydroxysuccinimide (NHS) and the common coupling agent *N,N′*-dicyclohexylcarbodiimide (DCC). The resulting active intermediate reacted with ammonium-modified chitosan **C1** to give the Pt-loaded conjugate **C12**. Different amounts of Pt(IV) complex and different reaction times were employed in this study (see Appendix A: Tables A1 and A2) in order to select the best compromise in terms of reaction time and amount/cost of Pt(IV) prodrug. As detailed in the experimental section, the loading conditions produced a **C12** conjugate containing 35.2 ± 6.0 µmol Pt g^{-1} chitosan (mean of three independent experiments). These were chosen to maximize the Pt loading in relatively short reaction times, and to limit the amount of **2** that was used in the syntheses.

Prodrug **2** was chosen based on previous studies where it was loaded on amino-functionalized nonporous silica nanoparticles resulting in conjugates with high cellular uptake and good antitumor activity [35,36]. Moreover, the presence of only one axial carboxylate functionality prevents the formation of cross-links between amino groups of different **C1** molecules decreasing the size of the nanoparticles [36]. Complex **2** is stable in HEPES buffer (HEPES = 4-(2-hydroxyethyl)piperazine-1-ethanesulfonic acid; pH = 7.5), but it can be reduced to cisplatin by bioreductants such as ascorbic acid (AA), with pseudo first-order initial rate constant $k = 1.2 \times 10^{-3}$ s^{-1} ($t_{1/2}$ = 9.4 h) and it was therefore released by the nanoparticles in the presence of AA, accordingly. To verify the behaviour of **2** loaded onto chitosan, conjugate **C12** was challenged with HEPES buffer (2 mM, pH = 7.5), with and without AA (see experimental section). In HEPES, the release of platinum was 2% over 48 h, whereas in the presence of AA, it reaches 48% in 8 h and 75% in 24 h. During the tests of antiproliferative activity, almost the whole Pt loading of chitosan may be released. In any case, it has been demonstrated that for such Pt(IV) prodrugs, the cytosolic content is able to completely and quickly reduce them to their Pt(II) active metabolite (in this case, cisplatin) [18,37,38].

After loading the Pt(IV) complex, the conjugate **C12** was further decorated with the tridentate ligand **3** using the above said coupling procedure with HBTU and DIPEA. Finally, the resulting conjugate **C123** was used to coordinate the *fac*-[Re(CO)$_3$]$^+$ core, by the reaction with *fac*-[Re^{I}Br$_3$(CO)$_3$][NEt$_4$]$_2$ with the known procedure at reflux in methanol [39,40], to give the conjugate **C1234**. The whole synthetic pathway is reported in Scheme 3.
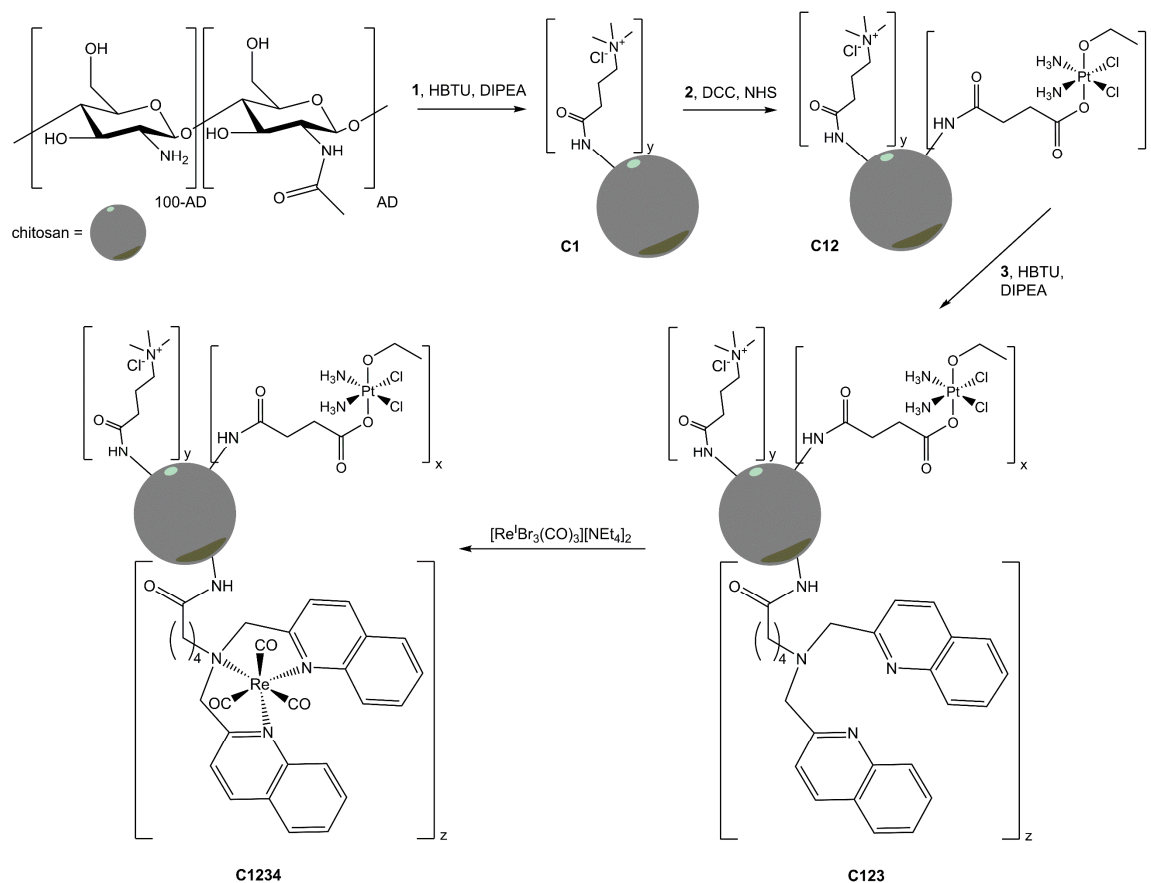

Scheme 3. Synthetic pathway from chitosan **C** to conjugate **C1234**. HBTU = *N,N,N′,N′*-tetramethyl-*O*-(1*H*-benzotriazol-1-yl)uronium hexafluorophosphate, DIPEA = *N,N*-diisopropylethylamine, NHS = *N*-hydroxysuccinimide, DCC = *N,N′*-dicyclohexylcarbodiimide.

After each reaction step, the size and the ζ-potential of the conjugates were checked (Table 1). Moreover, the Pt and Re content was determined with inductively coupled plasma-optical emission (ICP-OES) technique after mineralization of the samples: 34.8 ± 9.8 µmol Pt g^{-1} chitosan; 65.3 ± 12.1 mmol Re g^{-1} chitosan (mean of three independent syntheses). Finally, the IR spectrum of conjugate **C1234** showed two ν(C≡O) bands at 1895 and 2017 cm^{-1}, which are typical of the *fac*-[Re(CO)$_3$]$^+$ core; these bands appear at frequencies that are similar to those observed for the Re(I) tricarbonyl complex with ligand **3** (1902 and 2016 cm^{-1}, respectively).

Table 1. ζ-potential and dynamic light scattering (DLS) diameter for chitosan derivatives.

Compound	ζ-potential (mV)	DLS Diameter (nm)
C1	41.5 ± 3.1	180 ± 10
C12	37.5 ± 0.6	215 ± 12
C123	45.9 ± 1.1	298 ± 21
C1234	39.0 ± 2.4	300 ± 24

TEM (Transmission Electron Microscopy) analyses indicated that the nanoparticles are spherically shaped, with a diameter size averaging 35 nm, as exemplified for **C123** in Figure 1. The difference in the size of the conjugates between DLS (giving the hydrodynamic diameter by dispersing particles in aqueous phase) and TEM (giving the diameter of dried samples) analyses may be due to hydration and swelling of the samples in aqueous media, as well as to some degree of aggregation.
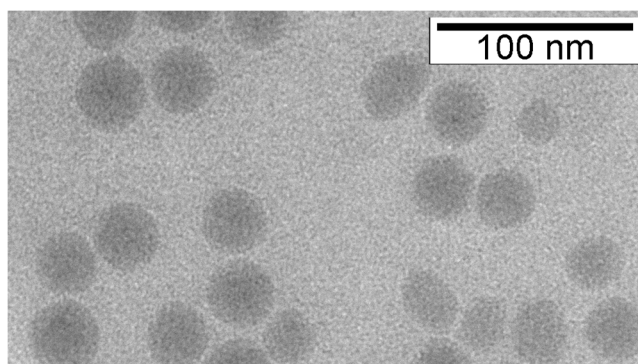
Figure 1. TEM image of **C123**.

2.2. Antiproliferative Activity and Cellular

To assess the cytotoxic activity of the different chitosan conjugates carrying the Pt(IV) prodrug, cancer cells were incubated for 48 h with increasing concentrations of the conjugates **C12**, **C123**, and **C1234**, and the cellular viability was evaluated by the 3-(4,5-dimethylthiazol-2-yl)-2,5-diphenyltetrazolium bromide (MTT) assay. This study was run in parallel for the **C1** chitosan platform and free Pt-complex **2**. The inhibition of growth (%) was calculated and the IC_{50} values were determined in mg·mL^{-1} for chitosan-containing particles, and in μM Pt concentrations for Pt-conjugates (Table 2). The ammonium-modified chitosan **C1** showed the lowest cytotoxicity with an IC_{50} value of 2.06 ± 0.83 mg·mL^{-1}. The monosuccinato Pt-complex **2**, although containing a free carboxylic group that could impart a low lipophilicity and reduce the cellular uptake, showed an antiproliferative activity of the same order of cisplatin (IC_{50}: 13.7 ± 3.0 and 20.7 ± 5.6 μM [41] for **2** and cisplatin, respectively). The linkage of the Pt(IV)-complex **2** to chitosan caused a slight increase of the cytotoxic activity of the nanosystems: the IC_{50} values were reduced from 2.06 (**C1**) to 1.34 mg·mL^{-1} (**C12**), although still being lower than that of complex **2** (33.7 vs. 13.7 μM, for **C12** and **2**, respectively). By contrast, the incorporation of the tridentate ligand **3** led to a chitosan-conjugate (**C123**) presenting an IC_{50} value (13.5 μM) similar to that found for the free Pt(IV) complex. These data are in clear contrast with the nanomolar IC_{50} values obtained for Pt(IV)-silica nanoparticles, carrying the same Pt(IV) prodrug [35,36]. Hence, it seems that the Pt(IV)-chitosan conjugation do not result in an improvement of the cytotoxic activity, namely when compared with cisplatin.

Table 2. Antiproliferative activity (IC_{50}) and accumulation ratio (AR) on A2780 cells.

Compound or Conjugate	IC_{50} (mg·mL^{-1}) [1]	IC_{50} (μM) [2]	Pt AR	Re AR
cisplatin	-	20.7 ± 5.6	-	-
2	-	13.7 ± 3.0	0.385 ± 0.091 [3]	
C1	2.06 ± 0.83	-	-	-
C12	1.34 ± 0.35	33.7 ± 8.9	3.56 ± 0.19	-
C123	0.43 ± 0.06	13.5 ± 2.0	-	-
C1234	0.65 ± 0.29	26.0 ± 11.8	2.31 ± 0.12	3.00 ± 0.87

IC_{50} values are expressed as: [1] mg·mL^{-1} of conjugate or [2] μM of Pt; [3] from refs. [35,36].

In the attempt to explain the poor antiproliferative activity of the conjugates, their cellular uptake was measured on A2780 human ovarian cancer cells. Cells were treated for 4 h with an external concentration of Pt between 6 and 8 μM, as checked by ICP-MS. The results of Pt and Re cellular accumulation were expressed in terms of the dimensionless accumulation ratio AR, i.e., the ratio between intra- and extra-cellular metal concentration. Conjugates **C12** and **C1234** showed AR values for both Pt and Re of about 3 (Table 2). These data seem to be quite low for metal drugs carried by macromolecular/nanoparticular vectors.

The scarce antiproliferative activity of the conjugates may have, therefore, its explanation in their corresponding low cellular accumulation. Generally, positively charged nanoparticles show higher uptake through endocytosis pathways than negatively charged counterparts, as observed for other Pt-loaded nanovectors of similar size and ζ-potential. In fact, spherical nonporous silica nanoparticles (NSNP) with an external shell containing primary amino groups were used as delivery systems for different Pt(IV) complex. The conjugates Pt(IV)-NSNP exhibited much better antiproliferative activity on the Pt-sensitive ovarian A2780 cell line than parent cisplatin and free complexes, due to their more efficient cellular uptake (in all cases AR > 30) [35,36]. On the contrary, phenanthriplatin (i.e., (*SP*-4-3)-diamminechlorido(phenanthridine)platinum(II) nitrate) loaded on negatively charged dextran sulfate, a polysaccharide not very different from chitosan, resulted in slightly less active than free phenanthriplatin. Also, in this case, the slightly lower AR (3.03 for conjugate vs. 4.81 for free complex) may justify this behavior [42]. Chitosan proved not to be an efficient carrier for the studied metal drugs: it increases the AR of the free Pt complex but it does not reach high levels. Very recently, mesoporous SNP (MSNP) functionalized with amino groups and then with hyaluronic acid (HA) or chitosan (**C**), showed very significant differences in terms of cellular uptake: MSNP-NH$_2$ and MSNP-HA were distributed in the cytoplasm of 3T3 mouse fibroblast cells, whereas MSNP-C were not able to penetrate the cells [43]. This result is in line with the data obtained in the current study.

3. Materials and Methods

3.1. General Procedures

K$_2$[PtCl$_4$] (Alfa Aesar-Thermo Fisher, Karlsruhe, Germany) and all other chemicals (Alfa Aesar-Thermo Fisher, Karlsruhe, Germany, and Sigma Aldrich Italia, Milan, Italy) were used without further purification. (*OC*-6-44)-diammine(4-carboxypropanoato)dichloridoethanolatoplatinum(IV) (**2**) was prepared and activated in its succinimidyl ester form, according to previously published procedure [35,36]. The ligand 5-[bis(quinolin-2-ylmethyl)amino]pentanoic acid (**3**) was synthesized, as described elsewhere [44]. Conductometric titrations were performed with a AMEL 160 conductivity meter and potentiometric titrations were performed with an AMEL 334-B pH meter (AMEL, Milan, Italy), both at 25.0 ± 0.1 °C by using a thermostatic circulating bath to keep the temperature of the sample constant. For the mineralization of the conjugates, 4–5 mg of product were mineralized by means of an acid digestion in 800 μL of 70% *w/w* HNO$_3$ using an ultrasonic bath at 60 °C for 1 h. The samples were then diluted with 1% *v/v* HNO$_3$. The Pt and Re content of the conjugates was quantified by means of inductively coupled plasma-optical emission spectrometry (ICP-OES), using a Spectro Genesis ICP-OES spectrometer (Spectro Analytical Instruments, Kleve, Germany) equipped with a crossflow nebulizer. In order to quantify the metal concentrations, the 299.797 nm and the 221.426 nm lines were used for Pt and Re, respectively. Platinum and rhenium standard stock solutions of 1000 mg·L^{-1} were diluted in 1% *v/v* nitric acid to prepare calibration standards. Particle size and ζ-potential were measured by dynamic light scattering (DLS) at 25 °C, at a fixed ionic strength, to compare the characteristics of the different particle samples, with a Malvern Zetasizer Nano ZS (Malvern Instruments Ltd., Malvern, UK) at a fixed scattering angle of 173°, using a He–Ne laser and DLS software for Windows (version 6.11, Malvern, UK). IR spectra (dry KBr plates, 2 cm^{-1} resolution) were recorded on a Bruker FTIR Equinox 55 spectrometer (Bruker Optik, Ettlingen, Germany) in the range 4000–400 cm^{-1}. Transmission electron microscopy (TEM) images were obtained on a JEOL

1400 (JEOL Ltd., Tokyo, Japan) instrument. TEM samples were prepared by placing 5 μL of gold nanoparticle solution on the 300 mesh carbon coated copper grid. Excess solution was removed carefully and the grid was allowed to dry for an additional five minutes. Pt and Re cellular content was measured by inductively coupled plasma-mass spectrometry (ICP-MS, Thermo Optek X Series 2, Thermo Scientific, Waltham, MA, USA). Instrumental settings were optimized in order to yield maximum sensitivity for platinum. For quantitative determination, the most abundant isotopes of platinum, rhenium, and indium (used as internal standard) were measured at m/z 195, 187 and 115, respectively.

3.2. Titrations: Deacetylation Degree of Chitosan

The quantification of the deacetylation degree (DD) of chitosan (i.e., of its amino groups) was carried with a conductometric titration [30]. In particular, 93.3 mg of chitosan were dissolved in 20 mL of 0.0540 M HCl and then the solution was titrated with 0.158 M NaOH, measuring the conductivity of the solution (mS·cm^{-1}) after each titrant addition. The data pointed out 5.16 mmol –NH$_2$ groups g^{-1} of chitosan, with an acetylation degree (AD) of 16.9 mol %. The corresponding potentiometric titration allowed for finding the pH ranges of solubility of chitosan: up to about pH 4 almost all of the amino functionalities are still protonated, whereas going on with the deprotonation (from pH around 4.5–5) chitosan started to precipitate and at neutral pH it was completely precipitated.

3.3. Synthesis of the Chitosan Modified with (3-Carboxypropyl)trimethylammonium Chloride (**C1**)

A mixture of (3-carboxypropyl)trimethylammonium chloride (**1**, 256 mg, 1.41 mmol), HBTU (803 mg, 2.12 mmol), and DIPEA (738 μL, 4.24 mmol) in 4 mL of anhydrous DMF was magnetically stirred for 30 minutes. Then, the protonated chitosan (228 mg, 1.18 mmol amine) and DIPEA (615 μL, 3.53 mmol) were added and the resulting mixture was stirred at room temperature for 24 h. The solvent was removed under reduced pressure and the product was dialyzed (dialysis tubing cellulose membrane with 14 kDa molecular weight cut-off) in ultrapure water for 2 d. After dialysis, the chitosan derivative was completely dissolved in water; then the sample was frozen with liquid nitrogen and lyophilized to get a beige powder. The amount of the ammonium derivative loaded on chitosan was quantified, as described above in Section 3.2. In particular, 21.0 mg of the sample were dissolved in 10 mL of 0.054 M HCl and titrated with 0.2 M NaOH by using a conductivity meter. The results showed that 29.5% of chitosan amino groups (1.52 mmol·g^{-1} of chitosan) was coupled with the ammonium derivative.

3.4. Loading of the Pt(IV) Complexes on Chitosan (**C12**)

To a suspension of **C1** in anhydrous DMF (228 mg of chitosan in 4 mL) prepared, as described in Section 3.3, activated complex **2** was added and the mixture was stirred. Different amounts of Pt(IV) complex and different reaction times were employed (see Appendix A: Tables A1 and A2) in order to select the best compromise in terms of reaction time and cost. After the established time, a small aliquot of the suspensions was processed: DMF was removed under reduced pressure and the conjugate was dialyzed in ultrapure water for 2 d, obtaining a completely water-soluble product. Then, few mg of the conjugate were frozen by means of liquid nitrogen, lyophilized, mineralized, diluted with 1% *v/v* HNO$_3$, and analyzed by means of ICP-OES to quantify the coordinated Pt. The use of 13.2 mg of activated **2** (i.e., 0.0236 mmol, corresponding to 2% respect to the total amino groups) and 4 h reaction time was chosen as standard loading conditions, producing conjugate **C12** containing 35.2 ± 6.0 μmol Pt g^{-1} chitosan (mean of three independent experiments).

3.5. Coupling of the Modified Chitosan Conjugate **C12** with the Ligand 5-[bis(Quinolin-2-ylmethyl)amino]pentanoic Acid, **3** (Conjugate **C123**)

A solution of the tridentate ligand **3** (9.1 mg, 0.0228 mmol), HBTU (13.0 mg, 0.0342 mmol) and DIPEA (7.94 μL, 0.0456 mmol) in anhydrous DMF (1 mL) was stirred for 30 minutes and then it was

added to the solution of **C12** in DMF (prepared as described in Section 3.4). The reaction was carried out at room temperature for 24 h. Then, DMF was removed under reduced pressure and the sample was recovered with ultrapure water, causing the precipitation of a dark brown powder (unreacted ligand), removed by extraction with dichloromethane. The aqueous phase (about 20 mL) was then dialyzed (MW cut-off membrane of 14 kDa) in ultrapure water for 2 d.

3.6. Chelation Reaction of Conjugate **C123** with the Re(I) Complex (**C1234**)

Fac-[ReBr$_3$(CO)$_3$][NEt$_4$]$_2$ (17.6 mg, 0.0228 mmol) was added to 10 mL of the dialyzed water solution of **C123** (see Section 3.5) and the reaction was let to proceed at 70 °C overnight. The solution was then dialyzed in ultrapure water for 2 d to separate the unreacted Re(I) tricarbonyl precursor from conjugate **C1234**. To determine the Pt and Re payloads of **C1234**, an aliquot of the final solution was frozen by liquid nitrogen and then lyophilized. The recovered **C1234** (4–5 mg) was mineralized by using the previously described method, diluted with 1% *v/v* HNO$_3$ and analyzed by means of ICP-OES to quantify the Pt and Re contents. The procedure was repeated at least three times. The Pt loading was 34.8 ± 9.8 μmol Pt g^{-1} chitosan ($0.68 \pm 0.19\%$ of the total amino groups), whereas the Re loading was 65.3 ± 12.1 μmol Re g^{-1} chitosan ($1.27 \pm 0.24\%$ of the total amino groups). IR (KBr): 1895 and 2017 cm^{-1}.

3.7. Solution Behaviour

Stability in pseudo-physiological conditions and reduction with ascorbic acid of **C12** (0.5 mM final Pt concentration) were studied in 2 mM 4-(2-hydroxyethyl)piperazine-1-ethanesulfonic acid (HEPES) buffer (pH = 7.5), with or without 5 mM ascorbic acid at different time intervals over 48 h at 25 °C. In particular, the spontaneous Pt leaking (i.e., in the absence of any reducing agents) was evaluated by considering conjugate **C12**. In particular, a concentrated HEPES buffer solution was added to an aliquot of the final aqueous solution of **C12** (see Section 3.4) to obtain a final 2 mM HEPES concentration (pH 7.5); the resulting solution was dialyzed against aqueous 2 mM HEPES (without refreshing the solution; membrane Molecular Weight Cut-off, MWCO = 14,000 u) for 48 h at 25 °C, in order to verify the spontaneous Pt release. After the fixed time, the whole dialyzed solution was lyophilized, mineralized, diluted with a known volume of 1% *v/v* HNO$_3$, and analyzed by ICP-MS. The residual Pt content was expressed as percent of the initial amount. A similar procedure was performed in the presence of ascorbic acid (10-fold molar excess respect to the platinum content), employing independent samples that were analyzed after different time intervals up to 48 h. In particular, ascorbic acid was added to different samples of the **C12** HEPES solution, which were stirred for the established time. Each solution was then dialyzed, refreshing the dialysis medium every 15 minutes to avoid a further detachment due to the presence of the reducing agent. Finally, the dialyzed solutions were lyophilized, mineralized, diluted with 1% *v/v* HNO$_3$, and analyzed by ICP-MS. Also, in this case, the residual Pt content was expressed as percent of the initial amount.

3.8. Antiproliferative Activity

The antiproliferative activity of the conjugates under investigation was assessed by the evaluation of their effects on cellular proliferation using the [1-(4,5-dimethylthiazol-2-yl)-2,5-diphenyl tetrazolium] (MTT) assay. Ovarian cancer A2780 cells were seeded in 96-well culture plates at a density of 2×10^4 cells per well, and were left to adhere overnight at 37 °C. Cells were then incubated with the conjugates at different dilutions (0–50 μM of Pt content) during 48 h at 37 °C and 5% CO$_2$. After incubation, the conjugates were removed and cells were washed with phosphate buffered saline (PBS, 200 μL). The cellular viability was assessed by incubating cells with MTT (200 μL of 0.5 mg·mL^{-1} solution in Modified Eagle's Medium without phenol red) during 3h at 37 °C. The MTT solution was removed and the insoluble and blue formazan crystals that formed were dissolved and homogenized with DMSO (200 μL per well). The absorbance of this colored (purple) solution was quantified by measuring the absorbance at 570 nm, using a plate spectrophotometer (Power

Wave Xs; Bio-Tek, Winooski, VT, USA). A blank solution was prepared with DMSO alone (200 μL per well). Each test was performed with at least six replicates. Inhibition of growth (%) was calculated by correlation with a control incubated without compound. IC50 values (i.e., concentration which reduces the growth by 50%) were determined using the Graph Pad Prism software and expressed in micromolar concentrations.

3.9. Cellular Uptake

Ovarian cancer A2780 cells, seeded in 10 mm Petri dishes, were treated with the conjugates under investigation ([Pt] between 6 and 8 μM) for 4 h in complete medium. At time zero, 100 μL of the medium was taken out from each sample to check the extracellular Pt concentration. At the end of the exposure, cells were washed three times with PBS, detached from the Petri dishes with 0.05% Trypsin $1\times$ and 2% EDTA (HyClone, Thermo Fisher, Karlsruhe, Germany), and harvested in fresh complete medium. An automatic cell counting device (Countess®, Life Technologies, Thermo Fisher, Karlsruhe, Germany) was used to measure the number and mean diameter of the cells. To analyze the cellular Pt and Re accumulation, the cells were transferred into a borosilicate glass tube and centrifuged at 1100 rpm for 5 min at room temperature. The main part of the supernatant was removed by aspiration, leaving about 200 μL to limit the cellular loss. Cellular pellets were stored at $-20\ ^{\circ}$C until mineralization. Once defrosted, 70% *w/w* HNO_3 (350 μL) was added to each sample, which was left 1 h at 60 $^{\circ}$C in an ultrasonic bath. Then, they were diluted with 1% *v/v* HNO_3 to a final 3% *v/v* acid concentration and were analyzed by means of ICP-MS to quantify the Pt and Re concentration. The cellular metal contents after drug treatment, normalized upon the cell number, was expressed as ng metal per 10^6 cells. From the measured mean cell diameter, the cellular volume was calculated for each sample to express cellular metal content in terms of molar concentration. Finally, the ratio between the intra- and extra-cellular (i.e., in the culture medium) concentrations was defined as the accumulation ratio (AR) [45,46].

4. Conclusions

In this work, the Pt(IV) complex (*OC*-6-44)-diammine(4-carboxypropanoato)dichloridoethanolatoplatinum(IV) and the Re(I) tricarbonyl complex of 5-[bis(quinolin-2-ylmethyl)amino]pentanoic acid, were conjugated to the polysaccharide carrier chitosan. DLS and zeta-potential measurements proved that the different nanoconjugates display zeta potential and hydrodynamic size values ranging between 37.5–45.9 mV and 215–300 nm. In particular, **C1234** shares similar physico-chemical properties with the chitosan nanoconjugate (**C12**), carrying only the Pt(IV) prodrug. Therefore, the presence of the Re(I) probe did not disturb the physico-chemical properties of the chitosan nanoplatform that was thought originally as a carrier to deliver the Pt(IV) prodrug. Moreover, the presence of the Re(I) tricarbonyl complex also did not compromise the albeit small cytotoxic activity of the Pt(IV)-containing chitosan nanosystems. Most importantly, these nanoplatforms can be equipped with imaging/diagnostic properties, namely by replacing the *fac*-$[Re(CO)_3]^+$ by the congener *fac*-$[^{99m}Tc(CO)_3]^+$ core.

The lower in vitro antiproliferative activity of **C1234** with respect to free **2** is due to the inefficient cellular uptake, as demonstrated by the accumulation ratio measurements. However, EPR effect increases extravasation and retention within the tumor tissue, but not necessarily within the tumor cells. For this reason, nanoparticles can be loaded with anticancer agents that accumulate and release their payload in the tumor environment, in the actual case, through activation by reduction. Therefore, the true active metabolite that will enter the cells may be the reduced Pt(II) active metabolite. Further in vivo tests will be necessary to appreciate any EPR effect for the conjugates to confirm the potential of the designed chitosan derivatives for the transport of anticancer agents.

Conflicts of Interest: The authors declare no conflict of interest.

Appendix

Table A1. Pt loadings on chitosan at different reaction times with a fixed amount of **2** (0.0236 mmol i.e., theoretical maximum % Pt loading = 2) (mean of three independent experiments). The results are expressed as percentage respect to the amino groups density (5.16 mmol·g^{-1} chitosan).

Conjugate	Reaction Time	Experimental % Pt Loading	μmol Pt g^{-1} Chitosan
C12a	2 h	0.78 ± 0.02	40.0 ± 0.9
C12b	4 h	0.68 ± 0.12	35.2 ± 6.0
C12c	6 h	0.86 ± 0.03	44.1 ± 1.5
C12d	8 h	0.61 ± 0.08	31.4 ± 3.9
C12e	24 h	0.99 ± 0.22	51.3 ± 11.2

Table A2. Pt loadings on chitosan at fixed reaction time (4 h) but by using different amounts of activated complex **2** (mean of three independent experiments). The results are expressed as percentage respect to the amino groups density (5.16 mmol·g^{-1} chitosan).

Conjugate	Theoretical Maximum % Pt Loading	Experimental % Pt Loading	μmol Pt g^{-1} Chitosan
C12f	1	0.45 ± 0.03	23.2 ± 1.5
C12b	2	0.68 ± 0.12	35.2 ± 6.0
C12g	5	1.38 ± 0.12	71.0 ± 6.2
C12h	10	2.63 ± 0.05	135.0 ± 0.3

References

1.　Kelland, L. The resurgence of platinum-based cancer chemotherapy. *Nat. Rev. Cancer* **2007**, *7*, 573–584. [CrossRef] [PubMed]

2.　Wheate, N.J.; Walker, S.; Craig, G.E.; Oun, R. The status of platinum anticancer drugs in the clinic and in clinical trials. *Dalton Trans.* **2010**, *39*, 8113–8127. [CrossRef] [PubMed]

3.　Apps, M.G.; Choi, E.H.Y.; Wheate, N.J. The state-of-play and future of platinum drugs. *Endocr. Relat Cancer* **2015**, *22*, R219–R233. [PubMed]

4.　Lammers, T.; Kiessling, F.; Hennink, W.E.; Storm, G. Drug targeting to tumors: Principles, pitfalls and (pre-) clinical progress. *J. Control. Release* **2012**, *161*, 175–187. [CrossRef] [PubMed]

5.　Stylianopoulos, T.; Jain, R.K. Design considerations for nanotherapeutics in oncology. *Nanomed. Nanotechnol. Biol. Med.* **2015**, *11*, 1893–1907. [CrossRef] [PubMed]

6.　Butler, J.S.; Sadler, P.J. Targeted delivery of platinum-based anticancer complexes. *Curr. Opin. Chem. Biol.* **2013**, *17*, 175–188. [CrossRef] [PubMed]

7.　Ma, P.A.; Xiao, H.H.; Li, C.X.; Dai, Y.L.; Cheng, Z.Y.; Hou, Z.Y.; Lin, J. Inorganic nanocarriers for platinum drug delivery. *Mater. Today* **2015**, *18*, 554–564. [CrossRef]

8.　Maldonado, C.R.; Salassa, L.; Gomez-Blanco, N.; Mareque-Rivas, J.C. Nano-functionalization of metal complexes for molecular imaging and anticancer therapy. *Coord. Chem. Rev.* **2013**, *257*, 2668–2688. [CrossRef]

9.　Kim, J.; Pramanick, S.; Lee, D.; Park, H.; Kim, W.J. Polymeric biomaterials for the delivery of platinum-based anticancer drugs. *Biomater. Sci.* **2015**, *3*, 1002–1017. [CrossRef] [PubMed]

10.　Massaguer, A.; Gonzalez-Canto, A.; Escribano, E.; Barrabes, S.; Artigas, G.; Moreno, V.; Marchan, V. Integrin-targeted delivery into cancer cells of a Pt(IV) pro-drug through conjugation to RGD-containing peptides. *Dalton Trans.* **2015**, *44*, 202–212. [CrossRef] [PubMed]

11. Wang, X.; Wang, X.; Guo, Z. Functionalization of platinum complexes for biomedical applications. *Acc. Chem. Res.* **2015**, *48*, 2622–2631. [CrossRef] [PubMed]

12. Johnstone, T.C.; Suntharalingam, K.; Lippard, S.J. The next generation of platinum drugs: Targeted Pt(II) agents, nanoparticle delivery, and Pt(IV) prodrugs. *Chem. Rev.* **2016**, *116*, 3436–3486. [CrossRef] [PubMed]

13. Wani, W.A.; Prashar, S.; Shreaz, S.; Gomez-Ruiz, S. Nanostructured materials functionalized with metal complexes: In search of alternatives for administering anticancer metallodrugs. *Coord. Chem. Rev.* **2016**, *312*, 67–98. [CrossRef]

14. Gabano, E.; Ravera, M.; Colangelo, D.; Osella, D. Bioinorganic chemistry: The study of the fate of platinum-based antitumour drugs. *Cur. Chem. Biol.* **2007**, *1*, 278–289.

15. Gabano, E.; Ravera, M.; Osella, D. The drug targeting and delivery approach applied to Pt-antitumour complexes: A coordination point of view. *Cur. Med. Chem.* **2009**, *16*, 4544–4580. [CrossRef]

16. Hall, M.D.; Mellor, H.R.; Callaghan, R.; Hambley, T.W. Basis for design and development of Platinum(IV) anticancer complexes. *J. Med. Chem.* **2007**, *50*, 3403–3411. [CrossRef] [PubMed]

17. Graf, N.; Lippard, S.J. Redox activation of metal-based prodrugs as a strategy for drug delivery. *Adv. Drug Deliv. Rev.* **2012**, *64*, 993–1004. [CrossRef] [PubMed]

18. Wexselblatt, E.; Gibson, D. What do we know about the reduction of Pt(IV) pro-drugs? *J. Inorg. Biochem.* **2012**, *117*, 220–229. [CrossRef] [PubMed]

19. Gianferrara, T.; Spagnul, C.; Alberto, R.; Gasser, G.; Ferrari, S.; Pierroz, V.; Bergamo, A.; Alessio, E. Towards matched pairs of Porphyrin-Re^I/^{99m}Tc^I conjugates that combine photodynamic activity with fluorescence and radio imaging. *ChemMedChem* **2014**, *9*, 1231–1237. [CrossRef] [PubMed]

20. Quental, l.; Raposinho, P.; Mendes, F.; Santos, I.; Navarro-Ranninger, C.; Alvarez-Valdes, A.; Huang, H.; Chao, H.; Rubbiani, R.; Gasser, G.; et al. Combining imaging and anticancer properties with new heterobimetallic Pt(II)/M(I) (M = Re, ^{99m}Tc) complexes. *Dalton Trans.* **2017**, *46*, 14523–14536. [CrossRef] [PubMed]

21. Moura, C.; Esteves, T.; Gano, L.; Raposinho, P.D.; Paulo, A.; Santos, I. Synthesis, characterization and biological evaluation of tricarbonyl M(I) (M = Re, Tc-99m) complexes functionalized with melanin-binding pharmacophores. *New J. Chem.* **2010**, *34*, 2564–2578. [CrossRef]

22. Can, D.; Spingler, B.; Schmutz, P.; Mendes, F.; Raposinho, P.; Fernandes, C.; Carta, F.; Innocenti, A.; Santos, I.; Supuran, C.T.; et al. (Cp-R)M(CO)$_3$ (M = Re or ^{99m}Tc) arylsulfonamide, arylsulfamide, and arylsulfamate conjugates for selective targeting of human carbonic anhydrase IX. *Angew. Chem. Int. Ed.* **2012**, *51*, 3354–3357. [CrossRef] [PubMed]

23. Leonidova, A.; Gasser, G. Underestimated potential of organometallic rhenium complexes as anticancer agents. *ACS Chem. Biol.* **2014**, *9*, 2180–2193. [CrossRef] [PubMed]

24. Leonidova, A.; Pierroz, V.; Rubbiani, R.; Heier, J.; Ferrari, S.; Gasser, G. Towards cancer cell-specific phototoxic organometallic rhenium(I) complexes. *Dalton Trans.* **2014**, *43*, 4287–4294. [CrossRef] [PubMed]

25. Kitanovic, I.; Can, S.Z.; Alborzinia, H.; Kitanovic, A.; Pierroz, V.; Leonidova, A.; Pinto, A.; Spingler, B.; Ferrari, S.; Molteni, R.; et al. A deadly organometallic luminescent probe: Anticancer activity of a ReI bisquinoline complex. *Chem. Eur. J.* **2014**, *20*, 2496–2507. [CrossRef] [PubMed]

26. Naik, A.; Rubbiani, R.; Gasser, G.; Spingler, B. Visible-light-induced annihilation of tumor cells with platinum-porphyrin conjugates. *Angew. Chem. Int. Ed.* **2014**, *53*, 6938–6941. [CrossRef] [PubMed]

27. Aranaz, I.; Harris, R.; Heras, A. Chitosan amphiphilic derivatives. Chemistry and applications. *Cur. Org. Chem.* **2010**, *14*, 308–330. [CrossRef]

28. Philippova, O.E.; Korchagina, E.V. Chitosan and its hydrophobic derivatives: Preparation and aggregation in dilute aqueous solutions. *Polym. Sci. Ser. A* **2012**, *54*, 552–572. [CrossRef]

29. Riva, R.; Ragelle, H.; des Rieux, A.; Duhem, N.; Jérôme, C.; Préat, V. Chitosan and chitosan derivatives in drug delivery and tissue engineering. In *Chitosan for Biomaterials II*; Jayakumar, R., Prabaharan, M., Muzzarelli, R.A.A., Eds.; Springer: Berlin/Heidelberg, Germany, 2011; Volume 244, pp. 19–44.

30. De Alvarenga, E.S.; de Oliveira, C.P.; Bellato, C.R. An approach to understanding the deacetylation degree of chitosan. *Carbohydr. Polym.* **2010**, *80*, 1155–1160. [CrossRef]

31. Casettari, L.; Vllasaliu, D.; Castagnino, E.; Stolnik, S.; Howdle, S.; Illum, L. PEGylated chitosan derivatives: Synthesis, characterizations and pharmaceutical applications. *Prog. Polym. Sci.* **2012**, *37*, 659–685. [CrossRef]

32. Sieval, A.B.; Thanou, M.; Kotze, A.F.; Verhoef, J.E.; Brussee, J.; Junginger, H.E. Preparation and NMR characterization of highly substituted *N*-trimethyl chitosan chloride. *Carbohydr. Polym.* **1998**, *36*, 157–165. [CrossRef]

33. Mohamed, N.A.; Sabaa, M.W.; El-Ghandour, A.H.; Abdel-Aziz, M.M.; Abdel-Gawad, O.F. Quaternized *N*-substituted carboxymethyl chitosan derivatives as antimicrobial agents. *Int. J. Biol. Macromol.* **2013**, *60*, 156–164. [CrossRef] [PubMed]

34. Domard, A.; Rinaudo, M.; Terrassin, C. New method for the quaternization of chitosan. *Int. J. Biol. Macromol.* **1986**, *8*, 105–107. [CrossRef]

35. Ravera, M.; Gabano, E.; Zanellato, I.; Perin, E.; Arrais, A.; Osella, D. Functionalized nonporous silica nanoparticles as carriers for Pt(IV) anticancer prodrugs. *Dalton Trans.* **2016**, *45*, 17233–17240. [CrossRef] [PubMed]

36. Ravera, M.; Perin, E.; Gabano, E.; Zanellato, I.; Panzarasa, G.; Sparnacci, K.; Laus, M.; Osella, D. Functional fluorescent nonporous silica nanoparticles as carriers for Pt(IV) anticancer prodrugs. *J. Inorg. Biochem.* **2015**, *151*, 132–142. [CrossRef] [PubMed]

37. Ravera, M.; Gabano, E.; Tinello, S.; Zanellato, I.; Osella, D. May glutamine addiction drive the delivery of antitumor cisplatin-based Pt(IV) prodrugs? *J. Inorg. Biochem.* **2017**, *167*, 27–35. [CrossRef] [PubMed]

38. Ravera, M.; Gabano, E.; Zanellato, I.; Fregonese, F.; Pelosi, G.; Platts, J.A.; Osella, D. Antiproliferative activity of a series of cisplatin-based Pt(IV)-acetylamido/carboxylato prodrugs. *Dalton Trans.* **2016**, *45*, 5300–5309. [CrossRef] [PubMed]

39. Alberto, R.; N'Dongo, H.P.; Clericuzio, M.; Bonetti, S.; Gabano, E.; Cassino, C.; Ravera, M.; Osella, D. Functionalized thymidine derivatives as carriers for the γ-emitter technetium tricarbonyl moiety. *Inorg. Chim. Acta* **2009**, *362*, 4785–4790. [CrossRef]

40. Alberto, R.; Egli, A.; Abram, U.; Hegetschweiler, K.; Gramlich, V.; Schubiger, P.A. Synthesis and reactivity of $[NEt_4]_2[ReBr_3(CO)_3]$. Formation and structural characterization of the clusters $[NEt_4][Re_3(\mu^3\text{-}OH)(\mu\text{-}OH)_3(CO)_9]$ and $[NEt_4][Re_2(\mu\text{-}OH)_3(CO)_6]$ by alkaline titration. *J. Chem. Soc. Dalton Trans.* **1994**, 2815–2820. [CrossRef]

41. Cardoso, J.M.S.; Correia, I.; Galvao, A.M.; Marques, F.; Carvalho, M. Synthesis of Ag(I) camphor sulphonylimine complexes and assessment of their cytotoxic properties against cisplcitin-resistant A2780cisR and A2780 cell lines. *J. Inorg. Biochem.* **2017**, *166*, 55–63. [CrossRef] [PubMed]

42. Ravera, M.; Gabano, E.; Zanellato, I.; Perin, E.; Arrais, A.; Osella, D. Polyanionic biopolymers for the delivery of Pt(II) cationic antiproliferative complexes. *Bioinorg. Chem. Appl.* **2016**, *2016*, 2380540. [CrossRef] [PubMed]

43. Salis, A.; Fanti, M.; Medda, L.; Nairi, V.; Cugia, F.; Piludu, M.; Sogos, V.; Monduzzi, M. Mesoporous silica nanoparticles functionalized with hyaluronic acid and chitosan biopolymers. Effect of functionalization on cell internalization. *Acs Biomater. Sci. Eng.* **2016**, *2*, 741–751. [CrossRef]

44. Viola-Villegas, N.; Rabideau, A.E.; Cesnavicious, J.; Zubieta, J.; Doyle, R.P. Targeting the folate receptor (FR): Imaging and cytotoxicity of Re–I conjugates in FR-overexpressing cancer cells. *ChemMedChem* **2008**, *3*, 1387–1394. [CrossRef] [PubMed]

45. Ghezzi, A.; Aceto, M.; Cassino, C.; Gabano, E.; Osella, D. Uptake of antitumor platinum(II)-complexes by cancer cells, assayed by inductively coupled plasma mass spectrometry (ICP-MS). *J. Inorg. Biochem.* **2004**, *98*, 73–78. [CrossRef] [PubMed]

46. Gabano, E.; Colangelo, D.; Ghezzi, A.R.; Osella, D. The influence of temperature on antiproliferative effects, cellular uptake and DNA platination of the clinically employed Pt(II)-drugs. *J. Inorg. Biochem.* **2008**, *102*, 629–635. [CrossRef] [PubMed]